





Python and GLO-DEM Pixel-Based Hypsometry in Upper **Indus Basin**

Rabia Qadir¹, Iqra Hameed¹, Aqsa Anwar², Saif Ullah Akhter³

¹Institute of Space Science, University of the Punjab, Lahore

²Institute of Geography, University of the Punjab, Lahore

³Department of Geography, Government Associate College, Eminabad, Gujranwala

*Correspondence: geotechs49@gmail.com

Citation | Qadir. R, Hameed. I, Anwar. A, Akhter. S. U, "Python and GLO-DEM Pixel-Based Hypsometry in Upper Indus Basin", IJIST, Vol. 07 Issue. 04 pp 2323-2337-, October 2025

Received | August 26, 2025 Revised | October 03, 2025 Accepted | October 05, 2025 Published | October 07, 2025.

orthern Pakistan's Hunza and Shyok headwaters, where the Karakoram, Himalaya, and Hindukush ranges converge, host some of the largest mid-latitude valley glaciers outside the polar regions and play a decisive role in runoff and hazards of the Upper Indus Basin. Hypsometry provides a rapid, terrain-based approach to assess basin condition in such high mountain settings. In this study, a 30 m digital elevation model was used to delineate 31 sub-catchments, and for each unit, the hypsometric curve and hypsometric integral (HI) were derived. Methods were kept consistent across scales, with HI also recalculated on 1-4 km grid tiles, and spatial organisation tested through Global Moran's I and the Getis-Ord Gi* statistic. Results reveal coherent belts of high HI aligned with the Main Karakoram Thrust, the Main Mantle Thrust, and the Karakoram Fault, indicating actively rising terrain and focused incision. Lower HI corridors occur in wider valley floors and recent fills, reflecting more mature landscapes and enhanced storage. HI distributions remain stable across tile sizes with mean values below one-half, while significant clustering confirms that these belts are intrinsic terrain signals. Harder crystalline and intrusive lithologies show higher HI on average, though wide variance suggests the combined influence of structure, rock strength, and relief. These geomorphic patterns carry direct hydrological meaning: high-HI belts imply fast translation of snow and ice melt with sharper seasonal peaks, whereas low-HI corridors favour storage and delay. Hypsometry, therefore, offers a cost-effective and reproducible tool for identifying active belts and providing priors for hydrological modelling and hazard planning in the Upper Indus Basin.

Keywords: Hypsometric Integral, Hypsometric Curve, Global Moran's I, Getis-Ord Gi* Statistic, Upper Indus Basin.











INFOBASE INDEX







ResearchGate













Introduction:

Northern Pakistan marks the confluence of three major mountain ranges, the Karakoram, Himalaya, and Hindukush. This unique convergence harbors some of the world's largest mid-latitude valley glaciers outside the polar regions and serves as a vital source for the Upper Indus Basin. An estimated 1,214 glaciers span approximately 12,705 square kilometers, with over 70% situated within the Karakoram region. In the upper Karakoram, the Hunza Basin governs the hydrology of multiple valleys, with elevations ranging from about 1,500 meters to over 7,500 meters above sea level. Iconic peaks such as Ladyfinger, Batura Muztagh, Shishper Sar, and Rakaposhi ring the basin and feed large ice bodies that act as natural reservoirs for downstream communities [1][2]. Snow and ice melt generated in these high mountain catchments can exceed one and a half times the outflow measured downstream along the Indus, which shows the scale of cryosphere control on water security for agriculture, energy, and settlements [3]. The Hindukush Himalaya cryosphere has been highly sensitive to recent global warming. Many glaciers have retreated or thinned, forming numerous morainedammed lakes near glacier termini whose sudden growth or failure can trigger glacial lake outburst floods that cascade into landslides, debris flows, and destructive flood waves. While the global picture is widespread retreat, parts of the Karakoram show relative mass stability and surge activity, a regional behavior often termed the Karakoram anomaly, which calls for basin-based evidence that links geomorphology, climate forcing, and hydrology rather than relying only on discharge trends [4][5][6]. Climate change modifies water resources by raising temperatures, shifting the timing and amount of snowfall and rainfall, and altering the onset and peak of melt seasons. The hydrology of the Upper Indus reflects the interaction of snow processes, glacier dynamics, and monsoon and westerly systems that vary across space and time. Observations indicate rising mean and extreme temperatures, shifting precipitation patterns, and increasing hazard frequency, all of which carry significant implications for livelihoods and infrastructure in Pakistan [7][8][9][10][11][12]. Regional institutions emphasize that a significant share of the global population relies directly or indirectly on mountain water, hydropower, timber, natural products, hazard mitigation, and recreation originating in the Hindu Kush and Himalaya. However, many valleys remain data sparse and require coordinated observations alongside local knowledge for practical adaptation [13][14]. The HKH spans tropical and subtropical influences at the foothills through to permanent ice and snow at the highest ridges. Warming during the twentieth century has been marked, with winter increases often exceeding other seasons, which affects snow cover duration, melt timing, and runoff character in headwater basins [15][16][17]. Pakistan ranks among the most climate-vulnerable countries due to its geography, heavy reliance on water and agriculture, limited adaptive capacity in certain regions, and gaps in disaster preparedness. Agro-climatic classifications further reveal that exposure and sensitivity vary across provinces and river basins [10]. In this context, hypsometry serves as a useful approach for interpreting the condition of a basin. The hypsometric curve and the hypsometric integral summarize how area is distributed with elevation and have long been used to compare watersheds and infer the imprint of tectonics, climate, and lithology. In the Karakoram and neighboring ranges, hypsometric analysis in a geographic information system has been used to examine watershed condition and to separate glaciated from non-glaciated responses in relation to slope, elevation, and rock type [18][19][20][21][22][23][11].

Pakistan spans the contact of the Eurasian plate in the north and the Indo-Pakistani plate in the south. In the north, the fold and thrust belts are divided into the Sulaiman belt and the northwestern Himalayan belt. The northern region comprises the Karakoram Terrane, the Kohistan Island Arc, and the Indo-Pakistan Plate, bounded by the Main Karakoram Thrust to the north and the Main Mantle Thrust to the south, which define the major tectonic contacts. The Hunza valley exposes rocks from Precambrian to recent age, including

metamorphic and volcanic units, and shows clear structural control on valley form, slope instability, and incision. The Main Karakoram Thrust hosts thick ophiolitic mélanges with serpentinite and volcanic rocks, while the Main Mantle Thrust marks the southern contact of the island arc against the Indian margin. Slope failures such as the Attabad event in January 2010 illustrate the hazard context created by steep slopes and active structures [24][25][26].

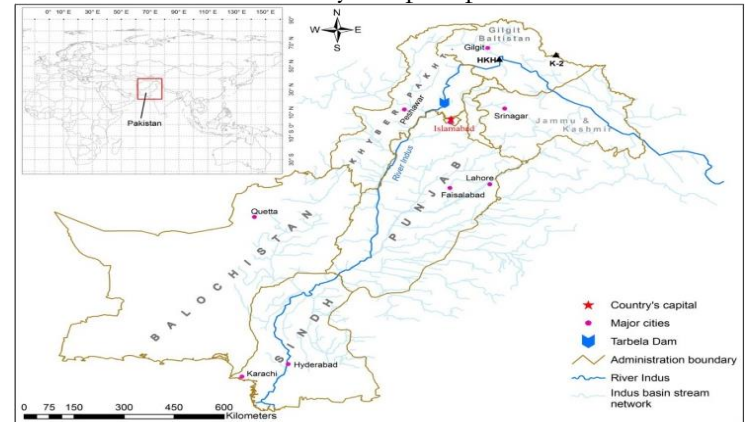


Figure 1. A map of Pakistan, presented with its provincial and administrative boundary lines. Five provinces are shown, namely Punjab, Sindh, Baluchistan, Khyber Pakhtunkhwa, and Gilgit Baltistan.

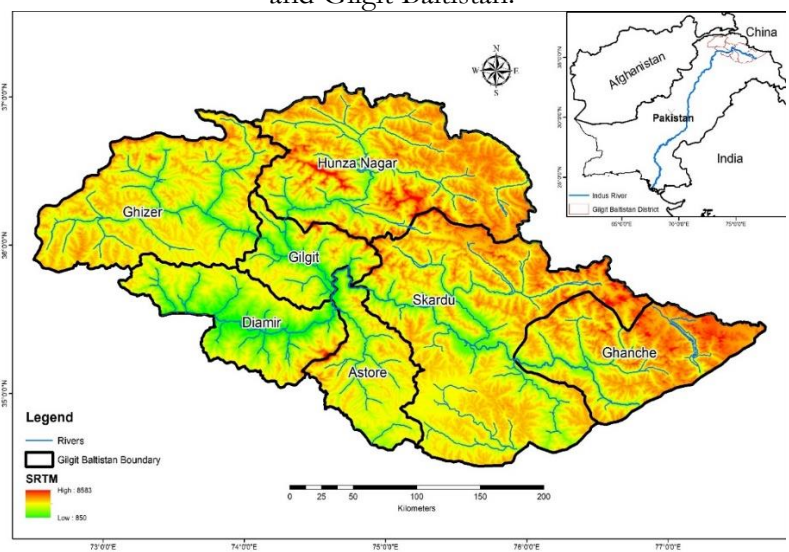


Figure 1. ASTER Global digital elevation model (GDEM) of Shyok and Hunza Basin, the location of UIB.

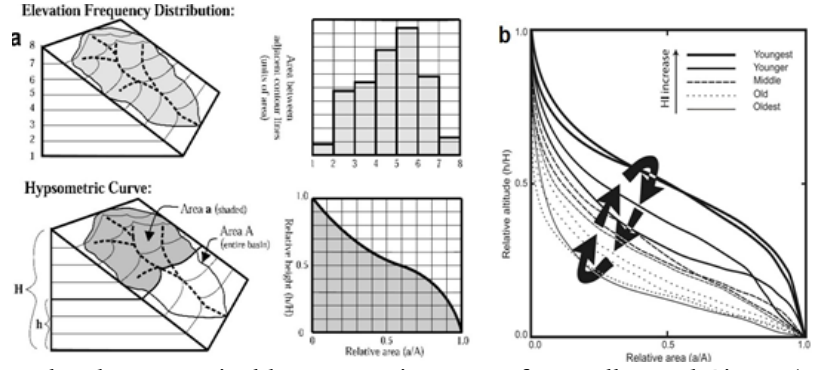


Figure 2. Panel a show a typical hypsometric curve after Keller and Pinter (2002. Panel b illustrates S-shaped and concave curves and their relation to medium and low hypsometric integral values, after Pérez Peña et al., 2009.



Objectives:

To compute pixel-based hypsometric integrals and curves across 31 sub-catchments of the Hunza-Shyok sector using a 30 m DEM, and to classify the basins into youthful, intermediate, and mature stages of landscape evolution.

To assess the spatial organisation of hypsometric signals through Global Moran's I and the Getis-Ord Gi statistic, and to interpret their geomorphic and hydrological significance in relation to lithology, tectonic structures, and meltwater response.

The novelty of this study lies in three aspects. First, unlike earlier basin-wide hypsometry in the region, we adopt a pixel-based approach, producing detailed maps that capture belts and corridors of contrasting geomorphic state. Second, we integrate *spatial statistics (Moran's I, Gi)* to assess clustering, an approach rarely applied in the Upper Indus context. Third, we explicitly link hypsometric belts to both lithology and active structures (Main Karakoram Thrust, Main Mantle Thrust, Karakoram Fault), and extend the interpretation to hydrological response and hazard management. Together, these contributions provide a reproducible and computational framework that advances hypsometry from descriptive indices to a decision-support tool for data-scarce mountain basins.

The present study first applies hypsometry as an organising lens to characterise youthful, mature, and old landscape patches [25][27][26] The study then relates hypsometric hot spots and cold spots to mapped structures, lithology, and storage zones within Hunza and Shyok. This provides the basis for modelling sections, where standard hydrological tools translate geomorphic signals into seasonal discharge and planning-relevant timing for the Upper Indus Basin [28][29][11].

Material and Methods:

Upper Indus River Basin:

The Indus is one of Asia's great rivers, originating in Tibet and flowing through India and Pakistan, with minor stretches in China and Afghanistan, before emptying into the Arabian Sea. The stretch from the headwaters to Tarbela is defined as the Upper Indus Basin (UIB). The river's main stem spans approximately 2,880 kilometres, draining nearly 912,000 square kilometres. Within this system, the operational UIB covers about 1,150 kilometres in length and roughly 165,400 square kilometres in area, aligning with regional hydrological delineations [30]. Click or tap here to enter text. Observation networks report fourteen high-elevation meteorological stations, nine lower-elevation weather stations, eleven hydrological stations, and up to eleven outflow stations that serve sub-basins such as Hunza, Shyok, Gilgit, Shigar, Astore, Zanskar, and Shingo, with a concentration in the northwestern sector [31]. Gilgit-Baltistan exhibits sharp climatic and relief gradients. Monsoonal influence diminishes toward the inner Karakoram and Hindukush, producing arid valley floors and cold high ridges. While valleys such as Astore, Khaplu, Yasin, Hunza, and Nagar remain cool during summer, areas like Gilgit and Chilas experience hot days with mild nights. Winters are widely subzero with summer maxima locally above forty degrees Celsius [16][22].

The geological framework spans the collision between the Eurasian plate and the Indo-Pakistan plate. The Karakoram terrane, the Kohistan Island arc, and the Indian margin meet along major structures, notably the Main Karakoram Thrust and the Main Mantle Thrust. The Shyok drainage encompasses portions of the Karakoram–Himalayan crystalline and thrust belts, as well as the Indus and Shyok suture zones. The region comprises marbles, amphibolites, gneisses, and metasediments, together with plutonic units of Ladakh and ophiolitic mélanges distributed along the suture strands. This structural grain governs valley orientation, relief, and slope instability in Hunza and Shyok. The present study centers on the Hunza and Shyok subcatchments because both contribute substantially to the Indus at their confluence, and any shift in the magnitude or timing of their flows influences water allocation, hydropower operation, and hazard exposure downstream. The Hunza is characterized by very

high relief, extensive glacier cover, and a complex litho-tectonic framework. The Shyok drains a large part of the Karakoram batholith and the suture zone and shows pronounced heterogeneity in glacier response across tributaries, which makes the pair a useful natural laboratory for basin comparison and for linking landscape metrics to hydrology [32][33][34][6]. The Hunza and Shyok basins form the focus of this study (Figure 4), which shows their location, main rivers, meteorological stations, and major tectonic structures critical for understanding basin form.

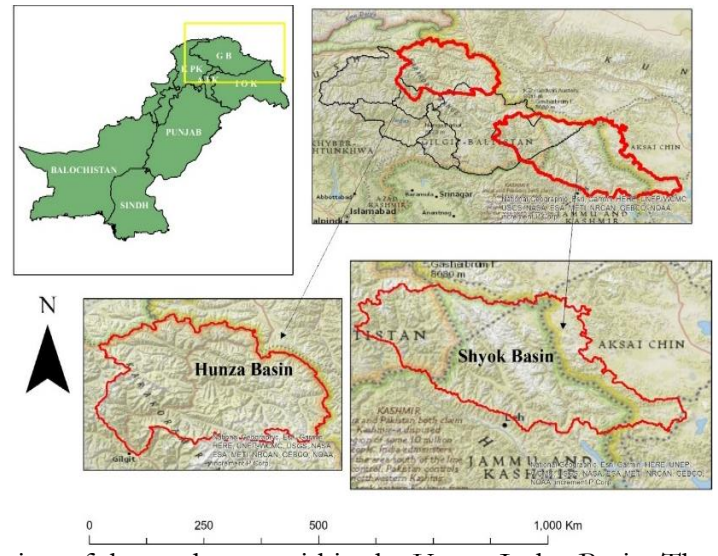


Figure 3. Location of the study area within the Upper Indus Basin. The map shows the Hunza and Shyok sub-basins outlined in red, which together form an important headwater region draining into the Indus River. The Hunza Basin lies in the western Karakoram, bounded by high peaks and extensive glaciers, while the Shyok Basin extends eastward across crystalline batholiths and suture zones. The inset map of Pakistan highlights the position of Gilgit-Baltistan and the adjoining northern ranges where the study area is located. Data Sources:

Terrain data were derived from the Shuttle Radar Topography Mission (~30 m resolution), reprojected to a common coordinate system, clipped to the Shyok-Hunza frame, and checked for voids. The dataset was retained at native resolution to preserve benches, scarps, and narrow valley floors in the hypsometric curves. Sub catchments were delineated hydrologically from this model and then adjusted against high-resolution satellite basemaps to avoid splits across hanging valleys and glacier tongues, producing the same 31 units used throughout the results. Structural and lithological context drew on published mapping of the Main Karakoram Thrust, the Main Mantle Thrust, and the regional Karakoram Fault, together with one to fifty thousand lithology for the Hunza-Shyok sector, used for interpretation and the lithology against hypsometry comparison rather than to condition the elevation model [32].

River center lines were extracted from the conditioned model to match sub catchment boundaries, satellite imagery supported visual checks of valley confinement and confluences, and hydro meteorological station records informed seasonal context without entering the hypsometry computations, which rely solely on terrain.

A thirty-meter Shuttle Radar Topography Mission digital elevation model served as the topographic base. The raster was projected to a common coordinate system, clipped to the study frame, and kept at native resolution for morphometric work. Voids, if present, were filled using a conservative interpolation approach. Small gaps were corrected through bilinear resampling, while larger gaps were addressed using spline interpolation. This ensured that genuine benches and scarps were preserved while maintaining continuity of the DEM surface.



Published vectors of the Main Karakoram Thrust, the Main Mantle Thrust, and the regional Karakoram Fault, combined with 1:50,000-scale lithological mapping, supplied the structural and lithological context for interpretation and for comparing lithology with hypsometry [32]. Click or tap here to enter text.

Hydrological Conditioning and Sub-Catchments:

Sink filling, D8 flow direction, and flow accumulation were generated from the DEM. Applying a uniform accumulation threshold yielded a drainage network that preserves valley confinement in high-relief terrain. Sub-catchments were delineated at major confluences, resulting in 31 units encompassing the Shyok and Hunza headwaters. Catchment boundaries were cross-verified with river maps and satellite basemaps to prevent artificial divisions across hanging valleys or glacier tongues. The identifiers, numbered 1 to 31, correspond directly to those used in the results figures. 2.3 Hypsometric workflow

Hypsometry describes the distribution of basin area with elevation and is typically represented by the hypsometric curve and the hypsometric integral [35][21][23][27]. Click or tap here to enter text. For each unit, elevations were normalized to relative elevation (h/H) and cumulative relative area (a/A), where H = %sub>max</sub> - %sub>min</sub>, h = % - %sub>min</sub>, h = % is the total area, and h = % represents the area above elevation h = %. The curve is the locus of an over A against h over H. The integral was computed in two equivalent ways for cross-check. First, the hypsometric integral was obtained through numerical integration of the curve using the trapezoidal rule. Second, it was calculated in its compact form.

$$HI = \frac{\bar{E} - E_{min}}{E_{max} - E_{min}} (1)$$

Where \bar{E} Is the mean elevation, E_{\min} is minimum, and E_{\max} is the maximum elevation of the basin.

Moran's I equation

$$I = \frac{N}{W} \cdot \frac{\sum_{i} \sum_{j} w_{ij} (x_i - \bar{x}) (x_j - \bar{x})}{\sum_{i} (x_i - \bar{x})^2}$$
(2)

Where

n = number of features

xi = value at location i

 \bar{x} = mean of all values

wij = spatial weight between features i and

Where: N = number of features, $x_i =$ value at location $i, \bar{x} =$ mean of all values, $w_{ij} =$

spatial weight between i and j, and $W = \sum_{i} \sum_{j} w_{ij}$.

Getis-Ord Gi* equation

$$G_{i}^{*} = \frac{\sum_{j} w_{ij} x_{j} - \bar{X} \sum_{j} w_{ij}}{s \sqrt{\frac{n \sum_{j} w_{ij}^{2} - (\sum_{j} w_{ij})^{2}}{n-1}}} (3)$$

Where:

xi = value at location i

xj = value at location j

wij = spatial weight between i and j

n = number of features

 $\backslash bar\{X\}$ = mean of all values

S = standard deviation of all x

with z^- bar zz^- as the mean elevation of the unit. An agreement within ± 0.01 was required, and larger discrepancies prompted a sampling check of the curve points. For mapping and for direct comparison with the results, the integral was binned into three classes that mirror the curve family and erosional stage observed in active mountain belts. Class I, representing a convex youthful form, is defined by an HI > 0.50. Class II, with an S-shaped intermediate form, corresponds to HI values between 0.30 and 0.50. Class III, indicating a concave mature form, is characterized by HI < 0.37. These thresholds reflect the spread found in this terrain and match the class legend used later. **Figure 5** illustrates the hypsometry concept, showing how convex curves indicate youthful relief, S-shaped curves reflect intermediate stages, and concave curves represent mature landscapes.

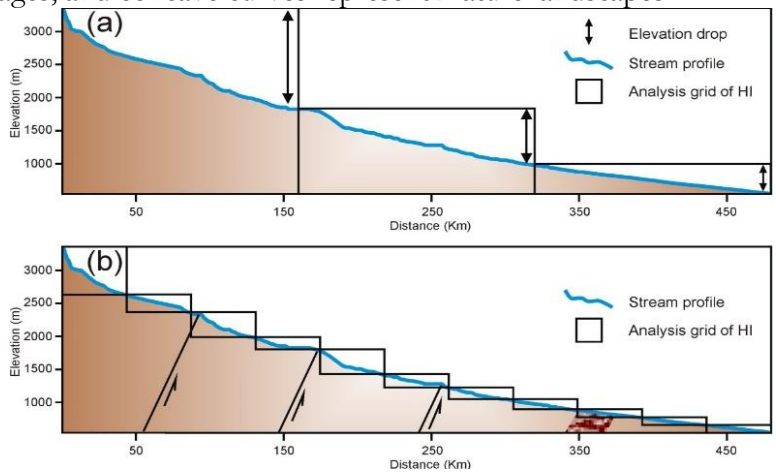


Figure 4. Hypsometry concept. Relative area and elevation curves and the integral. Convex curves with high values indicate youthful relief. S-shaped curves indicate intermediate balance. Concave curves with low values indicate mature to old landscapes.

Scale Testing and Spatial Statistics:

To test whether the mapped belts arise from inherent terrain features rather than unit scale, grids of 1-4 km were overlaid on the same area, and the hypsometric integral was recalculated for each tile using the 30 m elevation model. Skewness and kurtosis were calculated as curve moments to capture asymmetry and peakedness, complementing the visual classification of convex, S-shaped, and concave forms. Spatial patterns were further examined using Global Moran's I to test for clustering of the hypsometric integral, and the Getis-Ord Gi statistic to identify significant hot and cold belts. The parameters and tile sizes were kept consistent with those used in the distribution and moment plots, ensuring that the statistics correspond directly to the figures.

Lithology Linkage:

Lithology was simplified to seven strength classes that reflect dominant rock types reported in the map legends, from softer sedimentary packages to harder crystalline and intrusive bodies (Table 1). Each 1 km tile was assigned a lithology only if a single class occupied at least 90% of its area, thereby minimizing mixed signals. For these tiles, the mean hypsometric integral and its standard deviation were calculated for each class. The scatter plot presented later summarizes this relationship and supports the discussion on the combined influence of structure, rock strength, and relief [20][22].

Table 1. Lithology classes with representative rock types and strength category used for comparison with hypsometry

Class	Dominant Rock Types	Strength Category
I	Shale, claystone, marl	Very weak
II	Sandstone, siltstone	Weak
III	Limestone, dolomite, marble	Moderate



IV	Metasediments (phyllite, schist)	Moderately strong
V	Amphibolite, gneiss	Strong
VI	Granitic and other plutonic intrusives	Very strong
VII	Ophiolite, serpentinite, and volcanic units	Variable but strong

Quality Control:

No smoothing beyond sink filling was applied before hypsometry so that genuine benches and scarps remain visible in the curves. Visual checks against hill shade ensured that kinks in curves reflect terrain rather than striping or filling artefacts. Sub catchment identifiers remained fixed from data preparation through to plotting to prevent mismatches between text and plates. The integral from the compact form and from curve integration matched within tolerance across units. Stability of the belts across tile sizes was confirmed. Only belt width changes were noted with aggregation, which is expected when the grid size increases. The analytical workflow is summarized in Figure 6, which outlines the DEM processing, hypsometric analysis, and spatial statistics steps.

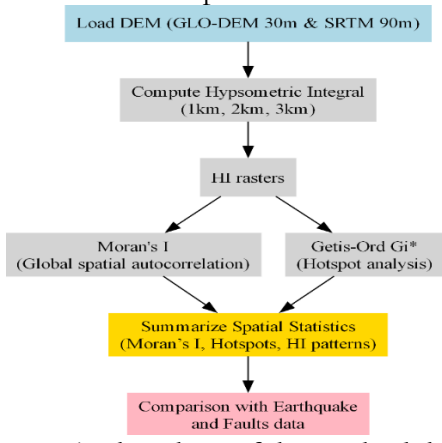


Figure 5. Flowchart of the methodology

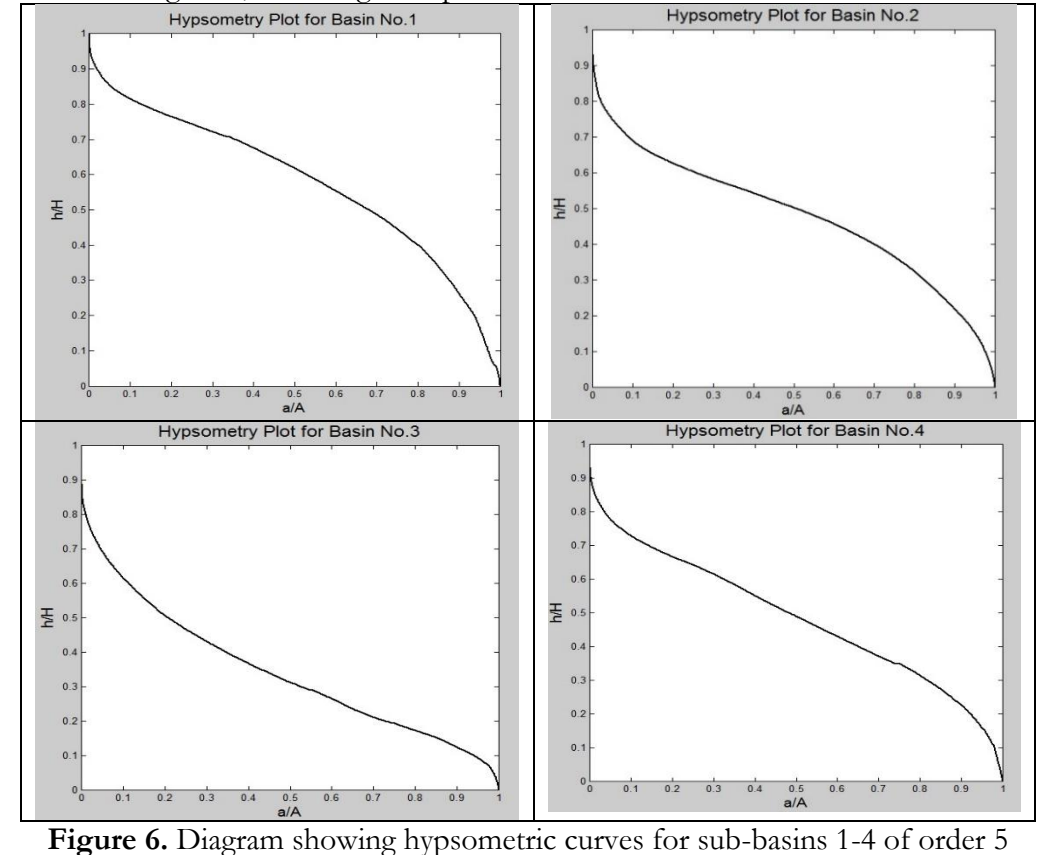
Result and Discussion: Results:

Hypsometric analysis of 31 sub-catchments in the Shyok and Hunza sector identifies three dominant curve families, each indicative of distinct stages of erosion. Convex curves with high hypsometric integrals dominate in 24 units, specifically 1-2, 4-6, 8-9, 12-15, and 17-29. These units retain large proportions of area at higher relative elevation and display strongly incised networks, indicating a youthful to actively rising terrain. Concave curves with lower integrals occur in 3, 7, 10-11, 16, and 30-31. These units present broader floors, gentler hillslopes, and more uniform drainage spacing, consistent with mature surfaces and enhanced storage. S-shaped curves mark transitional belts that sit between the two end members. Curve statistics support this reading. Positive skewness predominates in areas where uplift and incision are active, whereas occasional negative skewness reflects older-stage topography shaped by prolonged degradation. Spatial organization of the hypsometric signal is pronounced. High integral belts trace the mapped structural grain of the Main Karakoram Thrust and the Main Mantle Thrust and align with the regional trace of the Karakoram Fault, particularly along the northern and central tracts of Shyok and the eastern tracts of Hunza. Lower integral corridors occupy the northwestern and south-southeastern margins and follow wider valley floors downstream of major confluences. Global Moran's I confirm highly significant clustering of the hypsometric integral across all tested grid scales, while mean values remained below one half, demonstrating that the belt-corridor contrast is intrinsic to the terrain.

Lithology provides an important secondary control. A simplified seven-class scheme shows that harder crystalline and intrusive units tend to host higher mean integrals, whereas

softer sedimentary packages report lower means. The variance within each class is large, which indicates that rock strength alone does not govern the response; alignment with thrusts and shear zones enhances the effect in particular sub-basins. The combined pattern suggests joint control by structure, rock type, and relief.

Three figure plates carry the core signal from form to statistics to distribution. The panel of representative hypsometric curves shows convex, S-shaped, and concave forms for selected sub-basins and anchors the visual interpretation. The statistical moments consolidate this reading by placing each basin in a skewness-kurtosis field. The distribution plots of the integral across analysis tiles demonstrate stability of the signal across scale and show clear separation between high and low belts. Representative hypsometric curves are shown in Figure 7 to demonstrate how basin shape corresponds with HI values. Statistical moments are summarised in Figure 8, while Figure 9 presents HI distributions across scales.



Statistical Moments of Hypsometric Curves

| Hypsometric Inspect |

Figure 7. Statistical moments of hypsometric curves for basins 1–31. Positive skewness clusters along uplift-controlled belts; occasional negative skewness marks older stage surfaces.

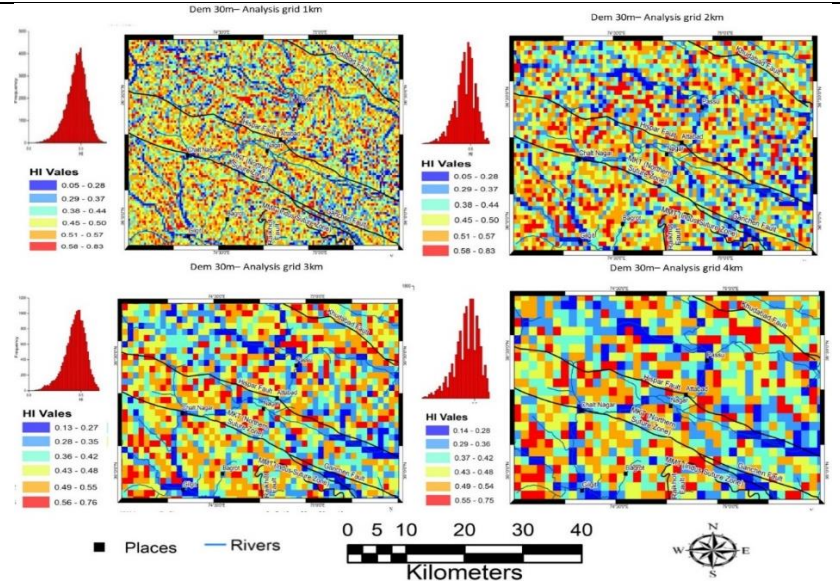


Figure 8. Distributions of the hypsometric integral computed from a thirty metre DEM for one-, two-, three- and four-kilometre tiles. Means remain below one-half with consistent separation between high and low belts across scales.

For completeness and for direct use in screening and planning, a single map plate is added that shades the hypsometric classes across all numbered sub-basins. A second map overlays the hot integral belt on the main structures to make the structural alignment explicit. A compact scatter plate then summarizes the relation between lithologic class and mean integral with standard deviation bars. The relationship between lithology and HI is summarized in **Figure 10**, where harder crystalline units tend to have higher HI compared to softer sedimentary packages.

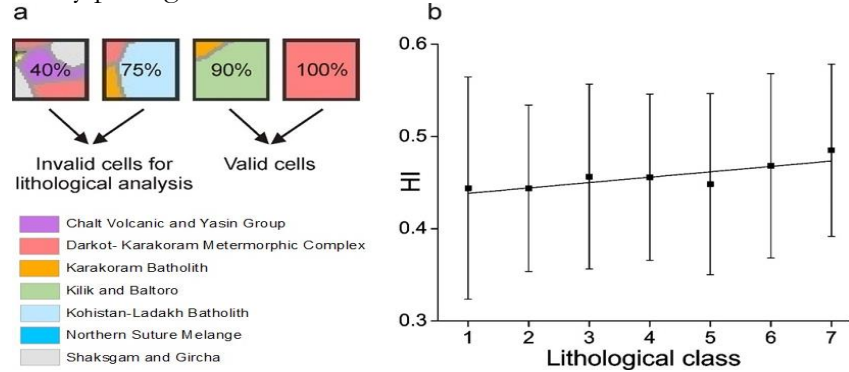


Figure 9. Figure 4.39. (a) Diagram showing the procedure for the selection of valid and invalid cells for the lithological analysis. (b) Mean HIVs extracted from 30 m DEM with an analysis grid of 1 km for each lithologic group (as shown in Table 1). The size of the error bar shows the standard deviation for the mean HI for each lithology class. Modified from Mahmood and Gloaguen, 2011.

Discussion:

The clustering of high integrals along the Main Karakoram Thrust, Main Mantle Thrust, and Karakoram Fault suggests that hypsometry is capturing zones of active uplift where neotectonic processes maintain steepened channel networks and elevated surfaces. This supports the interpretation that structural control, rather than lithology alone, governs basin form in these headwaters. Such alignment has also been noted in other active mountain belts, where hypsometric indices serve as reliable indicators of differential uplift and incision, e.g., [36][20]. In hydrological terms, these belts represent fast-response zones where snow and glacier melt are quickly transmitted to the main Indus River, increasing flood peaks.



Conversely, low-HI corridors indicate storage zones that delay runoff and may buffer peak discharges. This interpretive contrast goes beyond descriptive alignment and shows how geomorphology translates into hydrological behavior. Lower integral corridors step onto wider floors and recent valley fills that function as temporary storage for snowmelt and fine sediment. This staging accords with classic treatments where the hypsometric curve and integral act as indicators of erosional maturity and relief organization, and where convex forms with high integrals signal youthful or actively rising terrain, S shaped forms signal equilibrium like conditions, and concave forms with low integrals signal mature to old landscapes [18][21][23][27].

Comparative evidence from regional and global studies strengthens this reading. Work in the western Himalaya and Karakoram reports that high integrals frequently cluster along active structures and over resistant units, while mature basins over softer packages trend toward lower integrals and concave curves; the present lithology against integral relation is consistent with this composite control, even with large scatter in unit response [20][22]. Studies that tested scale effects of hypsometry found stability against practical variations in digital elevation model resolution but continued sensitivity to relief breaks and drainage organization. The present distributions across one-to-four-kilometer tiles and the significant clustering statistics agree with that pattern and add basin-specific confirmation for the Upper Indus sector [36][20].

The hydrological reading follows naturally. High integral belts contain steep gradients, narrow contributing hillslopes, and short travel paths, which favor fast translation of snow and ice melt and amplify seasonal peaks, a trait widely reported for glacierized Karakoram subbasins. Low-integral corridors have broad floors and storage zones that attenuate peaks and shift timing. This contrast is compatible with observed variability across the Hindukush-Karakoram-Himalaya and with the Karakoram anomaly, where discharge alone cannot diagnose glacier health and trend and where basin form and elevation distribution provide needed context for melt-driven regimes[32][11]. The belt map, therefore, offers a practical screening layer for route optimization, siting of assets, and early warning, while also providing a reproducible, computer-based indicator that fits the scope of the International Journal of Innovations in Science and Technology.

Methodological robustness is central to journal standards. The integral definition follows a simple normalized form, the curve families match standard geomorphic reading, and the tile-based evaluation avoids bias from irregular basin size. Stability of the belts across tile sizes and strong spatial autocorrelation at conventional confidence underscore that the signal is intrinsic to the terrain and not a product of processing. The scatter within lithologic classes is expected in a high-relief, glacier-influenced setting, where local uplift rate, debris cover, aspect, and valley confinement interact with rock strength. This scatter does not weaken the main inferences; rather, it identifies candidate reaches where field checks, geodetic rates, or borehole records would add value.

Finally, the approach remains compatible with the hydrological modelling sections planned for the full thesis. Hypsometric classes can be translated into prior information for parameter zoning in degree-day or energy balance frameworks, and into rule-based masks for routing calibration. Such integration is particularly useful where station networks are sparse and where the melt season contains most of the variance, as established for Hunza and Shyok.

Conclusion:

This article used hypsometry to read the Hunza and Shyok headwaters in a way that links elevation distribution, structure, and glacier cover to runoff pathways and hazards in the Upper Indus Basin. Three consistent outcomes emerge. First, belts with high hypsometric integrals and convex curves align with the Main Karakoram Thrust, the Main Mantle Thrust, and the regional Karakoram Fault, which indicates youthful to actively rising terrain with

steepened channel networks and rapid conveyance. Second, corridors with low integrals and concave curves occupy wider floors and recent valley fills and function as storage reaches that delay and attenuate meltwater. Third, these contrasts are not artefacts of processing. Curve statistics, significant spatial clustering, and stability across one-to-four-kilometer tiles confirm that the signal is intrinsic to the terrain. The computational workflow is simple and reproducible within a geographic information system. A thirty-meter elevation model, standard curve construction, integral estimation, and scale testing through tiles provide a transparent pipeline that is suited to data-sparse mountain basins. The lithology comparison shows that harder crystalline and intrusive units tend to retain higher integrals, yet the wide variance across classes points to joint control by structure, rock strength, and relief. In a high mountain setting where glacier debris, aspect, and confinement also matter, this behavior is expected and helps to identify corridors where targeted field checks and geodetic rates would add value.

The findings have direct practical meaning for Pakistan. High integral belts identify zones where seasonal snow and ice melt translate quickly to the river, which is relevant for flood preparedness, route planning, and the siting of critical infrastructure along the Karakoram Highway. Low integral corridors indicate places where storage and delay are likely, which is relevant for allocation decisions and for the placement of small reservoirs and protection works. Because the method is computational and relies on terrain alone, it aligns with the aims and scope of IJIST, where computer-based algorithms are used to generate scientific evidence that can support decision-making.

Important limits remain that a thirty-meter grid cannot resolve narrow benches or small moraine dams. Debris cover and short-term glacier surges are not represented explicitly. Lithology was simplified to seven classes to maintain coverage at the study scale. These limits suggest clear priorities for future work. Higher resolution elevation data, denser station networks, and integration with geodetic uplift and deformation will sharpen attribution. Companion papers can extend the same framework to drainage density, isobase levels, relative relief, and stream length gradients for a fuller structural reading. In summary, hypsometry offers a cost-effective and defensible first-order diagnosis of landscape state in the Shyok and Hunza basins. The belts and corridors identified here capture how structure, rock strength, and relief organize runoff and hazards in the Upper Indus. The maps and statistics are ready to be used as screening layers for planning and as priors in melt-driven hydrological models. This integrated, computer-based approach fits the IJIST emphasis on innovation in science and technology and provides basin-specific evidence that is immediately useful for water, energy, and risk management in Pakistan.

Acknowledgments:

The authors acknowledge the European Space Agency for the provision of GLO-DEM.

Author's Contribution:

R.Q. designed, conceptualized, and prepared the original draft. I.H. helped with manuscript drafting and methodologies. A.A. refined and assisted in DEM processing and execution of the Global Moran Index. S.U.A. did the supervision and Python execution.

Conflict of Interest: The Authors declare that there exists no conflict of interest in publishing this manuscript in IJIST.

References:

- [1] A. Ashraf, R. Naz, and R. Roohi, "Glacial lake outburst flood hazards in Hindukush, Karakoram and Himalayan Ranges of Pakistan: implications and risk analysis," *Geomatics, Nat. Hazards Risk*, vol. 3, no. 2, pp. 113–132, Jun. 2012, doi: 10.1080/19475705.2011.615344.
- [2] J. F. Shroder, N. Eqrar, H. Waizy, H. Ahmadi, and B. J. Weihs, "Review of the Geology of Afghanistan and its water resources," *Int. Geol. Rev.*, vol. 64, no. 7, pp.

- 1009–1031, Apr. 2022, doi: 10.1080/00206814.2021.1904297.
- [3] A. B. S. Francesca Pellicciotti, Cyrill Buergi, Walter Willem Immerzeel, Markus Konz, "Challenges and Uncertainties in Hydrological Modeling of Remote Hindu Kush–Karakoram–Himalayan (HKH) Basins: Suggestions for Calibration Strategies," *Mt. Res. Dev.*, vol. 32, no. 1, pp. 39–50, 2012, doi: https://doi.org/10.1659/MRD-JOURNAL-D-11-00092.1.
- [4] S. R. Bajracharya and B. Shrestha, "The Status of Glaciers in the Hindu Kush-Himalayan Region," 2011, doi: 10.53055/ICIMOD.551.
- [5] J. Birkmann and K. von Teichman, "Integrating disaster risk reduction and climate change adaptation: Key challenges-scales, knowledge, and norms," *Sustain. Sci.*, vol. 5, no. 2, pp. 171–184, May 2010, doi: 10.1007/S11625-010-0108-Y/METRICS.
- [6] B. Rasul, G., & Ahmad, "climate change in pakistan," *Pakistan Meteorol. Dep.*, 2012, [Online]. Available: https://scp.gov.pk/Conference2024/downloads/Climate_Chage_in_Pakistan.pdf
- [7] A. Amin *et al.*, "Regional climate assessment of precipitation and temperature in Southern Punjab (Pakistan) using SimCLIM climate model for different temporal scales," *Theor. Appl. Climatol.*, vol. 131, no. 1–2, pp. 121–131, Jan. 2018, doi: 10.1007/S00704-016-1960-1/METRICS.
- [8] (IPCC), "Climate Change 2022 Impacts, Adaptation and Vulnerability," *Intergov. Panel Clim. Chang.*, 2023, doi: https://doi.org/10.1017/9781009325844.
- [9] X. C. Yi Luo, Jeff Arnold, Shiyin Liu, Xiuying Wang, "Inclusion of glacier processes for distributed hydrological modeling at basin scale with application to a watershed in Tianshan Mountains, northwest China," *J. Hydrol.*, vol. 477, pp. 72–85, 2013, doi: https://doi.org/10.1016/j.jhydrol.2012.11.005.
- [10] H. A. & N. K. Sadia Mariam Malik, "Mapping vulnerability to climate change and its repercussions on human health in Pakistan," *Global. Health*, vol. 8, 2012, doi: https://doi.org/10.1186/1744-8603-8-31.
- [11] A. A. Tahir, P. Chevallier, Y. Arnaud, and B. Ahmad, "Snow cover dynamics and hydrological regime of the Hunza River basin, Karakoram Range, Northern Pakistan," *Hydrol. Earth Syst. Sci.*, vol. 15, no. 7, pp. 2275–2290, 2011, doi: 10.5194/HESS-15-2275-2011.
- [12] M. A. Nick Watts, "The 2018 report of the Lancet Countdown on health and climate change: shaping the health of nations for centuries to come," *Lancet*, vol. 392, no. 10163, pp. 2479–2514, 2018, [Online]. Available: https://www.thelancet.com/journals/lancet/article/PIIS0140-6736(18)32594-7/fulltext
- [13] N. Chettri *et al.*, "Changing Paradigm in Transboundary Landscape Management: A Retrospect from the Hindu Kush Himalaya," *Sustain. Dev. Goals Ser.*, vol. Part F2672, pp. 639–656, 2022, doi: 10.1007/978-3-030-70238-0_31.
- [14] S. G.-C. Stefan Schneiderbauer, Paola Fontanella Pisa, Jess L. Delves, Lydia Pedoth, Samuel Rufat, Marlene Erschbamer, Thomas Thaler, Fabio Carnelli, "Risk perception of climate change and natural hazards in global mountain regions: A critical review," *Sci. Total Environ.*, vol. 784, p. 146957, 2021, doi: https://doi.org/10.1016/j.scitotenv.2021.146957.
- [15] D. B. Meghnath Dhimal, "Impact of Climate Change on Health and Well-Being of People in Hindu Kush Himalayan Region: A Narrative Review," *Front. Physiol.*, 2021, doi: https://doi.org/10.3389/fphys.2021.651189.
- [16] M. A. Khan, J. A. Khan, Z. Ali, I. Ahmad, and M. N. Ahmad, "The challenge of climate change and policy response in Pakistan," *Environ. Earth Sci. 2016 755*, vol. 75, no. 5, pp. 1–16, Feb. 2016, doi: 10.1007/S12665-015-5127-7.

- [17] M. G. Thomas Kohler, "Mountains and Climate Change: A Global Concern," Mt. Res. Dev., vol. 30, no. 1, pp. 53–55, 2010, doi: https://doi.org/10.1659/MRD-JOURNAL-D-09-00086.1.
- [18] P. Edward, K. A., & Nicholas, "Active tectonics: earthquakes, uplift, and landscape," New Jersey Prentice Hall, 2022, [Online]. Available: https://www2.irsm.cas.cz/ext/ethiopia/materials/papers/tectonic_geomorphology/ Active tectonics_Keller_Pinter_small.pdf
- [19] J. Gilany, S. N. A., & Iqbal, "Geospatial analysis of glacial hazard prone areas of Shigar and Shayok basins," *Int. J. Innov. Appl. Stud.*, vol. 14, no. 3, p. 623, 2016, [Online]. Available: https://www.researchgate.net/publication/339148981_GEOSPATIAL_ANALYSIS _OF_GLACIAL_HAZARD_PRONE_AREAS_OF_SHIGAR_AND_SHAYOK_B ASINS
- [20] R. G. Syed Amer Mahmood, "Appraisal of active tectonics in Hindu Kush: Insights from DEM derived geomorphic indices and drainage analysis," *Geosci. Front.*, vol. 3, no. 4, pp. 407–428, 2012, doi: https://doi.org/10.1016/j.gsf.2011.12.002.
- [21] R. J. P. S. E. WILSON, "Elevation-Relief Ratio, Hypsometric Integral, and Geomorphic Area-Altitude Analysis," *Geol. Soc. Am. Bull.*, vol. 82, no. 4, pp. 1079–1084, 1971, [Online]. Available: https://pubs.geoscienceworld.org/gsa/gsabulletin/article/82/4/1079/7165/Elevation-Relief-Ratio-Hypsometric-Integral-and
- [22] J. Qureshi, S. A. Mahmood, A. Masood, P. Khalid, and I. S. Kaukab, "DEM and GIS-based hypsometric analysis to study tectonics and lithologies in southern Suleiman fold and thrust belt (Balochistan–Pakistan)," *Arab. J. Geosci.*, vol. 12, no. 5, pp. 1–15, Mar. 2019, doi: 10.1007/S12517-019-4283-6/METRICS.
- [23] S. A. SCHUMM, "EVOLUTION OF DRAINAGE SYSTEMS AND SLOPES IN BADLANDS AT PERTH AMBOY, NEW JERSEY," *Geol. Soc. Am. Bull.*, vol. 67, no. 5, pp. 597–646, 1956, [Online]. Available: https://pubs.geoscienceworld.org/gsa/gsabulletin/article/67/5/597/4811/EVOLU TION-OF-DRAINAGE-SYSTEMS-AND-SLOPES-IN
- [24] J. A. Dipietro, A. Hussain, I. Ahmad, and M. A. Khan, "The main mantle thrust in Pakistan: Its character and extent," *Geol. Soc. Spec. Publ.*, vol. 170, pp. 375–393, 2000, doi: 10.1144/GSL.SP.2000.170.01.20.
- [25] R. Khan, K., Ashraf, C. M., & Faridi, "Climate Change Effect On the Hunza Lake and Geomorphologic Status Of the Hunza River Basin, Gilgit-Baltistan, Pakistan," 14th World Lake Conf. Austin, 2011, [Online]. Available: https://www.pref.ibaraki.jp/soshiki/seikatsukankyo/kasumigauraesc/04_kenkyu/kai gi/docments/kosyou/14/2011wlc_Khalidakhan.pdf
- [26] D. G. Andrea Zanchi, "Multistage structural evolution of Northern Karakorum (Hunza region, Pakistan)," *Tectonophysics*, vol. 260, no. 1–3, pp. 145–165, 1996, doi: https://doi.org/10.1016/0040-1951(96)00081-9.
- [27] A. N. STRAHLER, "HYPSOMETRIC (AREA-ALTITUDE) ANALYSIS OF EROSIONAL TOPOGRAPHY," *Geol. Soc. Am. Bull.*, vol. 63, no. 11, pp. 1117–1142, 1952, [Online]. Available: https://pubs.geoscienceworld.org/gsa/gsabulletin/article/63/11/1117/4477/HYPS OMETRIC-AREA-ALTITUDE-ANALYSIS-OF-EROSIONAL
- [28] G. K. Devia, B. P. Ganasri, and G. S. Dwarakish, "A Review on Hydrological Models," *Aquat. Procedia*, vol. 4, pp. 1001–1007, 2015, doi: https://doi.org/10.1016/j.aqpro.2015.02.126.
- [29] M. A. Malik, A. Q. Dar, and M. K. Jain, "Modelling streamflow using the SWAT



- model and multi-site calibration utilizing SUFI-2 of SWAT-CUP model for high altitude catchments, NW Himalaya's," *Model. Earth Syst. Environ.*, vol. 8, no. 1, pp. 1203–1213, Mar. 2022, doi: 10.1007/S40808-021-01145-0/METRICS.
- [30] F. Garee, K.; Chen, X.; Bao, A.; Wang, Y.; Meng, "Hydrological Modeling of the Upper Indus Basin: A Case Study from a High-Altitude Glacierized Catchment Hunza," *Water*, vol. 9, no. 1, p. 17, 2017, doi: https://doi.org/10.3390/w9010017.
- [31] Z. Ahmad, M. Hafeez, and I. Ahmad, "Hydrology of mountainous areas in the upper Indus Basin, Northern Pakistan with the perspective of climate change," *Environ. Monit. Assess.*, vol. 184, no. 9, pp. 5255–5274, Sep. 2012, doi: 10.1007/S10661-011-2337-7/METRICS.
- [32] R. Bhambri, T. Bolch, P. Kawishwar, D. P. Dobhal, D. Srivastava, and B. Pratap, "Heterogeneity in glacier response in the upper Shyok valley, northeast Karakoram," *Cryosphere*, vol. 7, no. 5, pp. 1385–1398, 2013, doi: 10.5194/TC-7-1385-2013.
- [33] T. Kohler and D. Maselli, "Mountains and climate change: From understanding to action," 2009. Accessed: Oct. 03, 2025. [Online]. Available: https://lib.icimod.org/records/10dry-fv255
- [34] L. H. & L. X. Jingshi Liu, Shichang Kang, Kenneth Hewitt, "Large observational bias on discharge in the Indus River since 1970s," *Sci. Rep.*, vol. 8, 2018, doi: https://doi.org/10.1038/s41598-018-35600-3.
- [35] E. A. Keller and N. Pinter, *Active tectonics: earthquakes, uplift, and landscape*, 2nd ed. Upper Saddle River (N.J.): Prentice Hall, 2002.
- [36] Y. C. Chen, Q. Sung, and K. Y. Cheng, "Along-strike variations of morphotectonic features in the Western Foothills of Taiwan: tectonic implications based on streamgradient and hypsometric analysis," *Geomorphology*, vol. 56, no. 1–2, pp. 109–137, Nov. 2003, doi: 10.1016/S0169-555X(03)00059-X.



Copyright © by authors and 50Sea. This work is licensed under the Creative Commons Attribution 4.0 International License.